Preprint Author Copy - Vancostenoble, A., C. Duret-Thual, C. Bosch, and D. Delafosse. 2014. "Stress Corrosion Cracking of Cold Drawn Ferrito-Pearlitic Steels in Confined Aqueous Solutions Containing Dissolved CO2." In *NACE Corrosion Conference 2014*, 51314–4321–SG. Houston, Tx: NACE International. http://www.nace.org/cstm/Store/Product.aspx?id=762f2a5c-a5ba-e311-a396-0050569a007e.

Stress Corrosion Cracking of ferrito-pearlitic steel in aqueous environment containing dissolved CO_2

Alix Vancostenoble, Claude Duret - Thual
Institut de la corrosion
Site de Saint Etienne, Z.A. du Parc – secteur Gampille
42490 Fraisses
France

Cédric Bosch, David Delafosse
Ecole Nationale des Mines, SMS-EMSE, CNRS : UMR 5307, LGF
158 cours Fauriel
42023 Saint Etienne
France

ABSTRACT

A confined aqueous environment is defined by a very low water-volume to exposed steel-area ratio. In such media containing dissolved CO_2, siderite is formed and acts as a protective film. An addition of applied stress and/or environmental fluctuation can disturb the balance between the steel and this protective film, causing the fracture of the latter and leading to Stress Corrosion Cracking (SCC). The material studied is a cold drawn and rolled high strength steel composed of ferrite and spheroidized pearlite and has a strong microstructural anisotropy due to the specific cold work process. To investigate its susceptibility to SCC, Slow Strain Rate Tests (SSRT) were carried out on smooth and notched specimens allowing to separate crack initiation and crack propagation. The environment is an aqueous chloride solution saturated in CO_2 at pH around 6. Tests were performed under open circuit potential (OCP) and at cathodic potential. Under OCP, localized anodic dissolution in shear bands is responsible for crack initiation. Under cathodic potential, crack initiation is delayed due to the absence of critical defect on the surface. Both fractographic analyses and results obtained on notched specimens showed that hydrogen plays an important role in crack propagation.

Key words: Stress corrosion cracking, spheroidized pearlitic steel, hydrogen embrittlement

INTRODUCTION

Cold-drawn and cold-rolled ferrito-pearlitic steels are widely used for their high yield strength while a maintaining sufficient ductility for use as structural materials. However, like any carbon steel, they can suffer from uniform corrosion in aqueous solution. In de-aerated solution containing dissolved CO_2, the formation and precipitation of siderite ($FeCO_3$) as corrosion product depends on the temperature and the supersaturation level of Fe^{2+}.[1] These conditions can be met in a confined environment where the water-volume to steel-area ratio is very low and the content of ferrous ions is very high. As a consequence, the precipitated siderite at the surface acts as a protective film and reduces the corrosion rate.[2,3] Applying stresses and/or environmental fluctuations destabilize the protective layer, causing its fracture and leading to Stress Corrosion Cracking (SCC) damage. Moreover, the cold working process of pearlitic steel produces a strongly anisotropic microstructure

that could influence the SCC susceptibility and the mode of fracture. In many SCC phenomena, both anodic dissolution and hydrogen effects are involved and interact with the localized crack-tip plasticity. Experimentally, the respective roles of these processes are not easy to separate and require a methodology based on the mechanisms of corrosion-deformation interactions. An approach involves the use of micro-notched specimens subjected to dynamic deformation like Slow Strain Rate Tests (SSRT) to trigger the mechanisms at the notch tip and monitor them during the test. The control of the electrochemical and mechanical conditions allows exploring the key factors influencing damage.[4,5]
This methodology is applied to a high strength steel in a chloride solution saturated in CO_2. The mechanisms of SCC are investigated using slow strain rate tests on smooth and micro-notched specimens under different electrochemical conditions. The specific roles of anodic dissolution and hydrogen effects are particularly considered during the crack initiation and crack propagation.

EXPERIMENTAL PROCEDURE

The material studied was a cold-rolled and cold-drawn ferrito-pearlitic steel containing 0.3% of carbon. The steel was annealed after cold-working. As a consequence, the microstructure was constituted of spheroidized pearlite and recrystallized ferrite. The largest carbides are located along the boundaries between adjacent pearlite colonies and between these colonies and ferrite grains. The anisotropy of the microstructure produced by the cold work process is preserved despite the thermal treatment. Thus, it presents pearlite colonies elongated along the rolling direction (RD) (figure 1a) while in the transverse direction (TD), the microstructure is equiaxed (figure 1b).

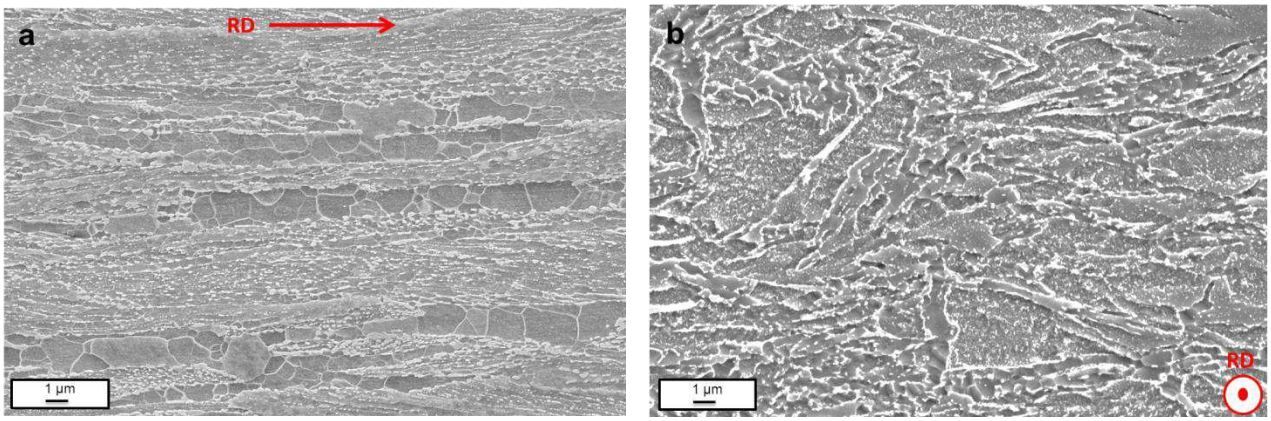

Figure 1: Microstructure of the steel: (a) rolling direction, (b) transverse direction.

SCC behavior was studied using Slow Strain Rate Tests (SSRT) on smooth and micro-notched specimens. Notched specimens were used in order to separate the specific roles of the anodic dissolution and hydrogen effect in the crack initiation and propagation mechanisms. The µ-notch provides a localized plastic zone that favors the corrosion-deformation interactions.[4,5]
Specimens were sampled along the rolling direction of the steel. The gage length and the cross-section were respectively 12 mm and 2.5x4 mm². Surfaces of specimen were polished with emery paper to a 1500 grit finish. The micro-notch was machined at mid-height of the gage length with a diamond wire saw to avoid any local strain hardening (figure 2). Smooth and notched specimens were tested respectively at a strain rate of $10^{-7}s^{-1}$ and $10^{-6}s^{-1}$.

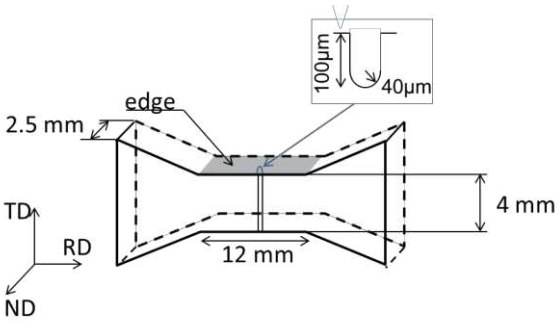

Figure 2: micro-notched specimen

The SCC tests were conducted in a corrosion cell with three electrodes, using a counter electrode in platinum and a saturated calomel electrode (SCE) connected to the cell with an external salt-bridge for the reference potential. Two electrochemical conditions were explored, at free potential in open circuit (OCP) and at cathodic potential (E_c = -1200 mV/SCE). Table 1 summarizes the composition of the solutions used and the potentials applied or measured. At OCP, the solution was confined by adding carbon steel coupons to saturate the solution with metallic cations. The ratio of water-volume to steel-area exposed to the solution, which measures the confinement of the solution, is equal to 0.3 mL/cm^2. In these conditions, the pH of the seawater solution saturated with CO_2 was 6.

Table 1
Environmental conditions applied during SSRT

At OCP (E_0 = -670 mV/SCE)	Under cathodic polarization (E_c = -1200 mV/SCE)
Synthetic seawater saturated in CO_2 confined solution (V/S=0,3 mL/cm^2) oxygen concentration < 5 ppb	Synthetic seawater saturated in CO_2 oxygen concentration < 20 ppb

An additional SSRT with a potential jump was performed. The test was started at OCP then the potential was shifted to E_c = -1200 mV/SCE at 5% elongation.
Fractographic analyses were performed on all the specimens after failure using a scanning electron microscope with field emission gun (SEM-FEG). Microstructures were observed on cross-sections etched with a 5% nital solution. The effect of environmental conditions was evaluated through the ratio of elongation-to-failure obtained in the test environment to that in air.

RESULTS

SSRTs on smooth specimens

Figure 3 shows stress *vs* elongation curves obtained on smooth specimens at free and cathodic potentials, compared with the reference test in air. Elongation-to-failure obtained for the two tests in aqueous environment is considerably reduced compared to the test in air. However, one notes a quick stress decrease after the Ultimate Tensile Stress (UTS) for at OCP, while at Ec some amount of stable necking is observed before the final fracture. In both cases, high plastic strains have to be applied in aqueous environment to trigger environmentally-assisted fracture.

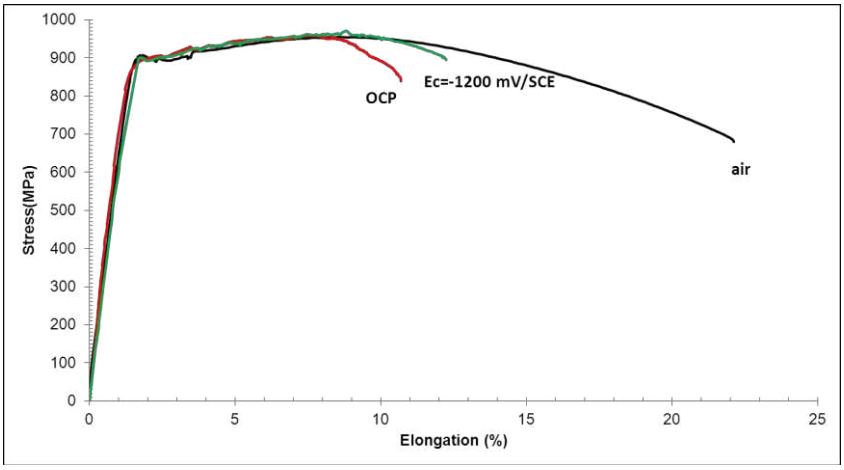

Figure 3: Stress-elongation curves on smooth specimens

Fractographic observations on the reference specimen tested in air reveal a fracture surface constituted of ductile tearing and longitudinal delaminations (figure 4a). These delaminations results from brittle crack propagations in the rolling direction (which is also the tensile direction). The longitudinal delaminations in the center are surrounded by a region of ductile tearing characterized by the presence of dimples (figure 4b). Delaminations occur both along boundaries between adjacent pearlite colonies where the largest carbides are located, and along ferrite/pearlite colony interfaces (figure 5).

Under cathodic polarization (CP), no main delamination was observed at mild-thickness in the specimen (figure 6). Conversely, numerous small longitudinal delaminations were observed, which initiated from the lateral edges of the sample and propagated towards the center. The initiation sites seem to be shear bands which emerge at the surface. The others parts of the fracture surface show ductile shearings and are very similar to those observed in air.

At OCP, these small longitudinal delaminations located at the lateral edges of the smooth specimen are also observed (figure 7a). The difference with previous results is that at free potential, initiation sites in shear bands are also sites of preferential dissolution (figure7b). This can promote earlier crack initiation compared to tests at cathodic potential.

Figure 8 presents a cross section of the specimen close to the fracture surface showing dissolved shear bands which act as critical defects for crack initiation. The very thin crack tip to less than 20 µm from the surface suggests that two different mechanisms operate for crack initiation and crack propagation. The former obviously involves anodic dissolution, while hydrogen may play a role in the latter.

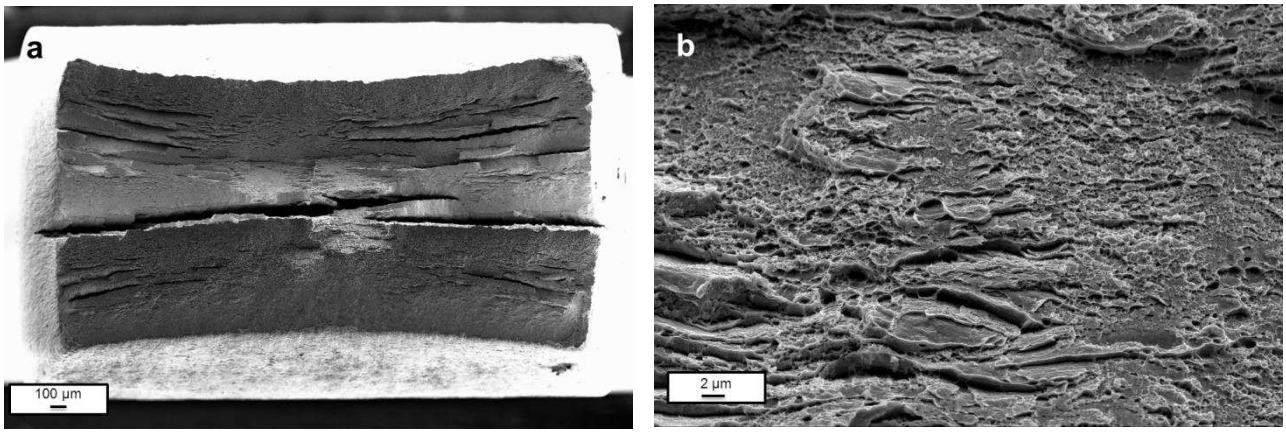

Figure 4: (a) Fracture surface of reference specimen tested in air, and (b) magnification of tearing and dimples in a ductile region,

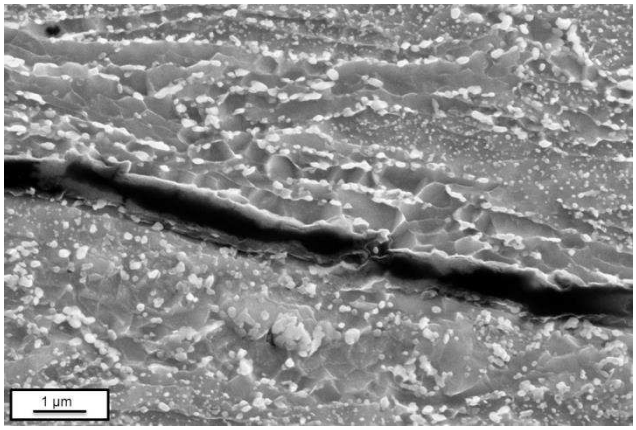

Figure 5: Longitudinal delamination along carbides on metallographic cross section observed close to the fracture surface of reference specimen tested in air.

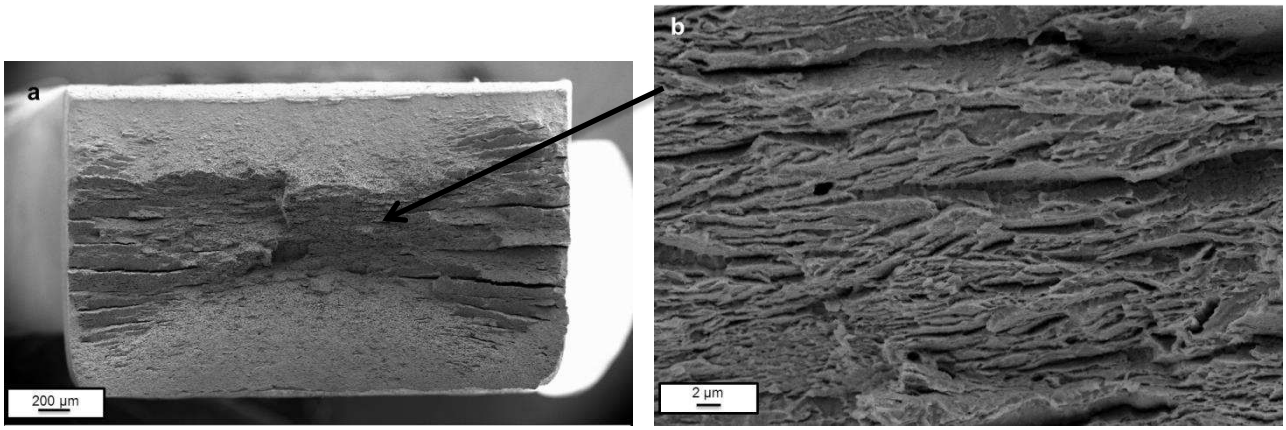

Figure 6: (a) Fracture surface of specimen tested under CP, and (b) magnification on the numerous longitudinal small delaminations

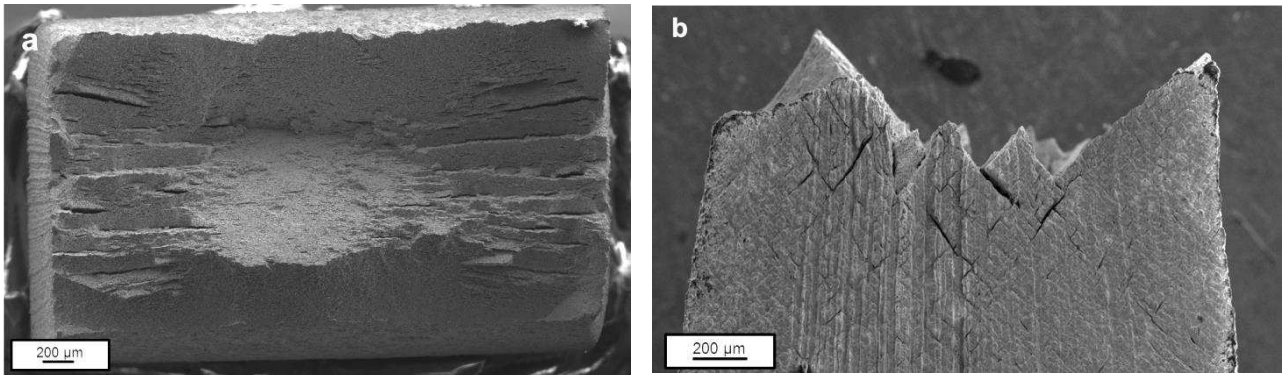

Figure 7: (a) Fracture surface of specimen tested at OCP, and (b) preferential dissolution of shear bands on the lateral surface.

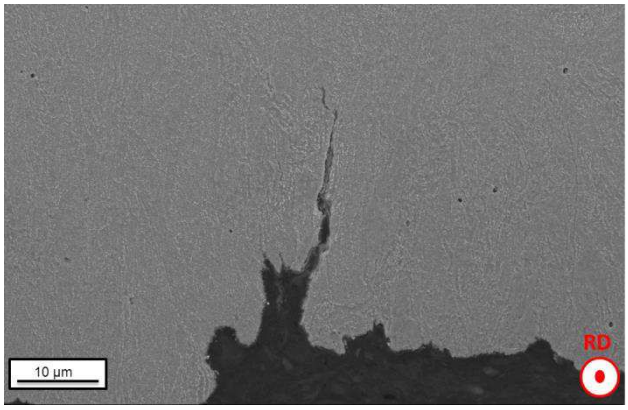

Figure 8: Cross-section of specimen tested at OCP. Notice that the crack tip very thin and the dissolved shear band acts as a critical defect for crack initiation.

SSRTs on notched specimens

Figure 9 shows stress *vs* elongation curves obtained from SSRTs on the micro-notched specimens. Here again, tests in aqueous environment show premature damage to the steel. Unlike the previous results on smooth specimens, elongation-to-failure is smaller under cathodic polarization than at free potential in open circuit conditions.

Preprint Author Copy - Vancostenoble, A., C. Duret-Thual, C. Bosch, and D. Delafosse. 2014. "Stress Corrosion Cracking of Cold Drawn Ferrito-Pearlitic Steels in Confined Aqueous Solutions Containing Dissolved CO2." In *NACE Corrosion Conference 2014*, 51314–4321–SG. Houston, Tx: NACE International. http://www.nace.org/cstm/Store/Product.aspx?id=762f2a5c-a5ba-e311-a396-0050569a007e.

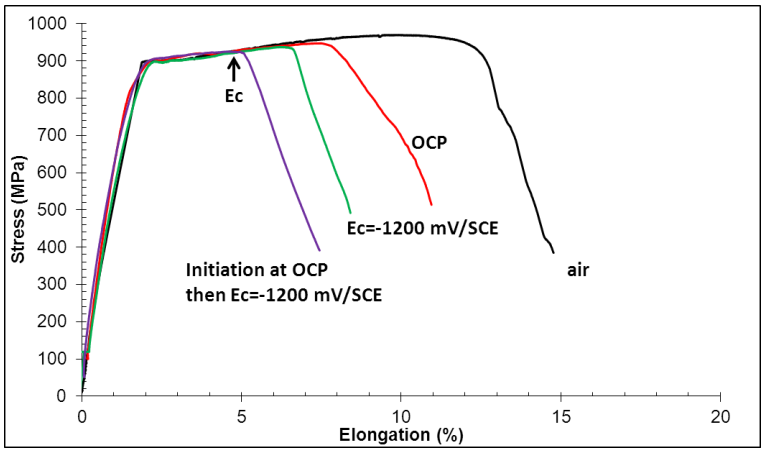

Figure 9 : Stress-elongation curves on micro-notched specimens

Fractographic investigations on the micro-notched specimen tested in air reveals a ductile fracture mode by shearing and some small longitudinal delaminations.
Under cathodic polarization, the fracture surface shows different features: a first brittle zone fractured by a pseudo-cleavage mode perpendicular to the loading direction (figure 10b); a second zone, just below the previous one, results from numerous short longitudinal delaminations and small ductile tearing (figure 10c); and a third region of shear ductile fracture, which caused the final fracture.

Observation on cross-sections close to the fracture surface has revealed several micro-voids which nucleated at cementite/ferrite interfaces. The comparison between specimens tested in air and under CP, shows that the number and the size of these micro-voids are higher under CP than in air as illustrated in figure 11.

Preprint Author Copy - Vancostenoble, A., C. Duret-Thual, C. Bosch, and D. Delafosse. 2014. "Stress Corrosion Cracking of Cold Drawn Ferrito-Pearlitic Steels in Confined Aqueous Solutions Containing Dissolved CO2." In *NACE Corrosion Conference 2014*, 51314–4321–SG. Houston, Tx: NACE International. http://www.nace.org/cstm/Store/Product.aspx?id=762f2a5c-a5ba-e311-a396-0050569a007e.

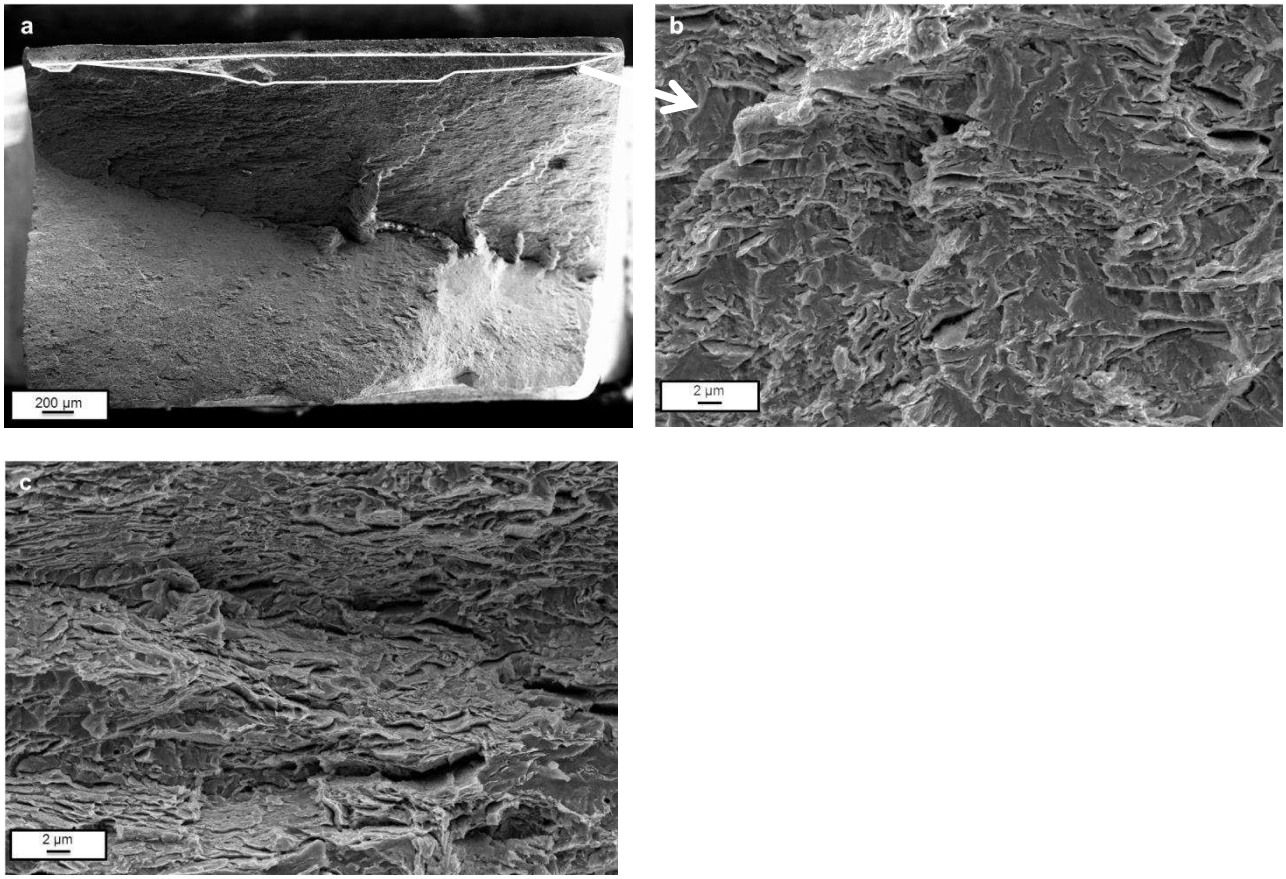

Figure 10: (a) Fracture surface of specimen tested under CP, (b) magnification of the first brittle zone ahead of the notch tip, (c) second zone with numerous small delaminations and ductile tearing.

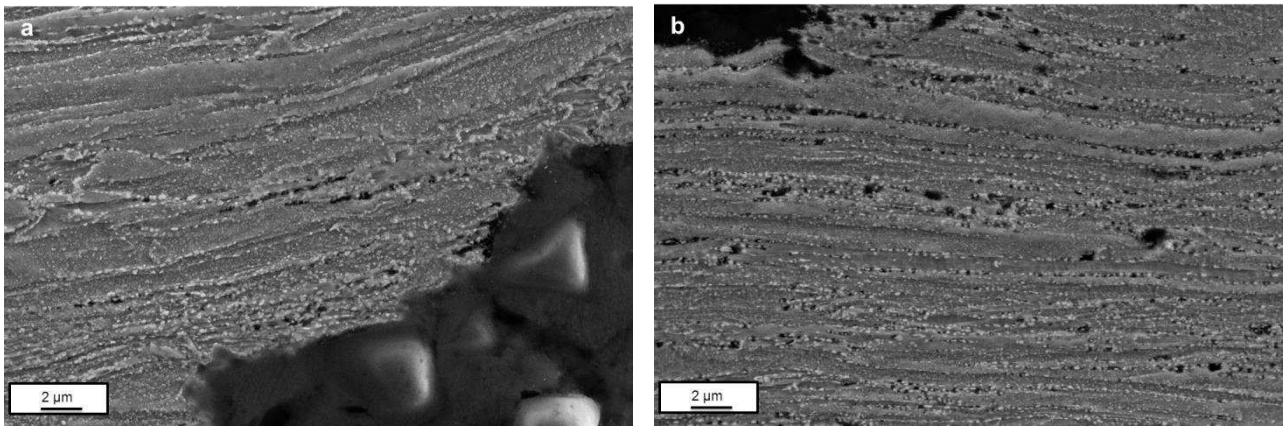

Figure 11: Cross-section of specimens observed in the rolling direction and close to the fracture surface, (a) tested in air, and (b) under CP.

At OCP, the fracture surface is marked by the anodic dissolution (figure 12a). Close to the notch tip, it is characterized by numerous longitudinal delaminations and small ductile tearings (figure 12b). A region of final fracture by ductile shearing is still present.

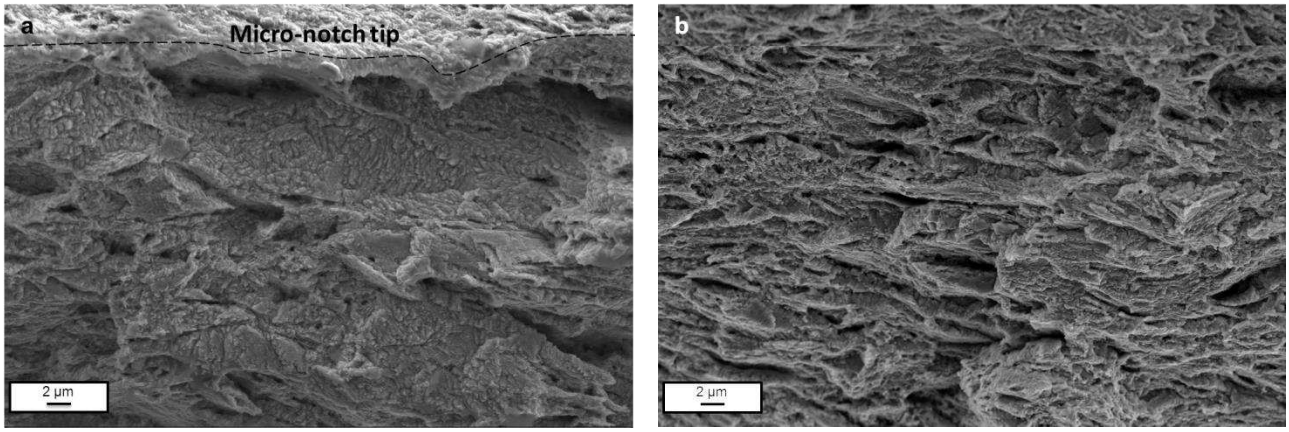

Figure 12: (a) Magnification of the fracture surface of specimen tested at OCP close to the notch tip, and (b) Fracture zone resulting from numerous longitudinal small delaminations and small ductile tearing.

The SSRT which started at OCP before shifting the potential to a cathodic value at 5% elongation gave the lowest elongation to rupture. The failure occurred very quickly after the change in potential.

The fracture surface is shown on figure 13. The region nearest to the notch tip is similar to that observed at OCP (figure 13a). It is characterized by numerous longitudinal delaminations and small ductile tearing with traces of anodic dissolution. A second zone following the previous shows a brittle region with a cleavage-like appearance, similar to that observed under CP (figure 13b). Finally, the third one is the final fracture surface showing the ductile shearing.

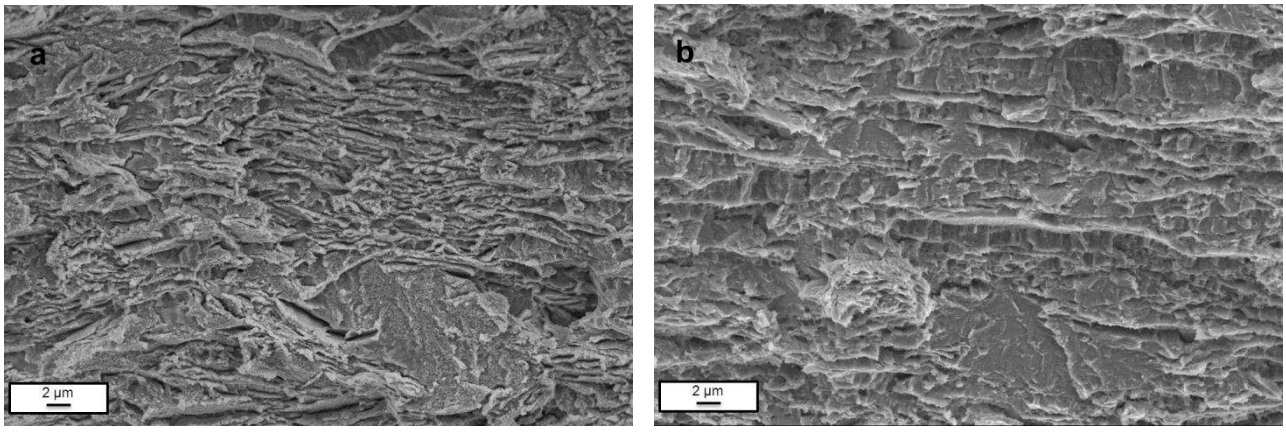

Figure 13: Fracture surface of the specimen tested with a jump of potential from OCP to CP. (a) Magnification close to the notch tip, and (b) further from the first, corresponding to mode of fracture under CP.

DISCUSSION

Tensile curves on smooth specimens have shown that environment affects the ductility only at high plastic strains, typically after the UTS when the mechanical damage process begins to operate. This process involves

the formation and coalescence of microvoids at ferrite/cementite interfaces. The preferential sites of void nucleation are the largest carbides of cementite located on the boundaries of adjacent pearlite colonies. Ultimately, growth and coalescence of microvoids lead to the longitudinal delaminations because of both the anisotropic microstructure (the larger carbides are aligned with the rolling direction which is also the tensile direction) and the triaxiality of stresses which increases with the beginning of the necking. This process is illustrated in figure 11a where the hydrostatic stress is increased at the notch tip.

Under CP, hydrogen is introduced into the material by electrolytic charging and is trapped at the metallurgical sites (precipitate/ferrite interfaces, grain boundaries, dislocations …) weakening the steel by different possible mechanisms. The microscopic events leading to failure seem to be unchanged compared to the reference test in air on smooth specimens. These features are consistent with those described in literature.[6,7,8] Indeed, several authors have studied the effect of hydrogen on spheroidized pearlitic steels but the mechanism of hydrogen embrittlement is still not clear. Cialone explained that more microvoids could be formed for a given macroscopic elongation, leading to failure at lower macroscopic elongation with the increase of hydrogen concentration in the neck.[6] Garber showed that hydrogen does not affect the nucleation or the growth of microvoids but accelerates the coalescence process.[9] It is well established that hydrogen diffuses towards the locations of maximum triaxial-stress in the material, due to the lowering of the chemical potential. The high local concentration of hydrogen present within the necking zone, where the triaxial-stress state is maximized, could assist the growth and coalescence of microvoids. This explains both the increasing number of longitudinal small delaminations observed on the fracture surface and the microvoids size observed on metallographic sections.
The results obtained on micro-notched specimens under CP have shown brittle facets corresponding to cleavage-like cracking. This suggests that localized plasticity is necessary to observe a significant hydrogen effect. A critical hydrogen concentration is achieved in the location of the maximum triaxial stress state causing early crack propagation. In this case, microvoids could act as nuclei for cleavage facets.

At OCP, fractographic analyses suggest that anodic dissolution plays a key role in the crack initiation. The emergence of shear bands at the surface produces preferential sites of dissolution caused by a slip-dissolution type of process. However, this process does not seem to be involved in crack propagation. The slip dissolution model postulates that dynamic plastic strain at the crack tip can break a protective film, allowing a burst of metal dissolution prior to repassivation; repetition of this sequence extends the crack.[10] Nevertheless at OCP, no trace of dissolution has been observed at the crack tip as illustrated in figure 8. Therefore, another mechanism must be responsible for the crack propagation. Considering the cathodic discharge of hydrogen, accompanied by the anodic dissolution in this de-aerated environment, the ingress of hydrogen into the steel and its effects might be involved in the mechanism of embrittlement.
On micro-notched specimens, the localized anodic dissolution process is sufficient to initiate a crack. Indeed, the fractographic surface is highly marked by anodic dissolution close to the notch tip driving by the high local strain. Just after this zone, the fracture surface is characterized by numerous longitudinal small delaminations, and this cannot be explained only by a dissolution process. The characteristic features of this region are similar to those observed under CP, which suggests that hydrogen plays a role in the crack propagation even at OCP. Hydrogen produced by electrochemical reaction at the crack tip surface, is absorbed in the material and diffused ahead of the crack tip where there is a high concentration of stress and local plastic strain. A critical local concentration of hydrogen could be reached and cause early crack initiation at the critical defect produced by dissolution.

The SSRT started at OCP and then switched to cathodic potential supports these results. At OCP, the crack is initiated by anodic dissolution, dissolution rate being accelerated and localized at the notch tip. The crack has a sharper tip than the artificial micro-notch machined on the specimen. The sharpness has an influence on the local plasticity at the crack tip, which consequently leads to a higher hydrogen concentration. For the same hydrogen concentration more stress is necessary to trigger crack propagation at a blunt crack tip.[11] After the stage at OCP, a high plastic strain region is localized at the crack tip. In this local plastic area the hydrogen

concentration increased when the potential was shifted to a negative value and caused the cleavage-like cracking at lower strain and stress than that obtained with the notched specimen subjected to SSRT under CP.

CONCLUSIONS

The mechanisms of stress corrosion cracking of a cold drawn and rolled high strength steel in a de-aerated chloride solution saturated in CO_2 have been explored using a methodology based on the corrosion-deformation interactions.[4]

At free potential, crack initiation occurs on sites of preferential dissolution, which are all sites of strain localization, and in particular, shear bands emerging at the surface. The localized dissolution on these sites creates critical surface defects from which cracks are initiated.

Hydrogen does not take part in the crack initiation process at OCP. A brittle cleavage-like cracking occurs when a critical content of hydrogen and a specific stress are reached ahead of the crack tip.

At cathodic potential, crack initiation from the micro-notch is delayed compared to that produced by anodic dissolution.

The sensitivity of the cold drawn and rolled high strength steel in de-aerated chloride solution to SCC in CO_2 is thus dependent on the presence and the geometry of surface defects. The preferential dissolution in shear bands promotes the formation of severe surface defects which increase the susceptibility to SCC.

REFERENCES

1. A. Dugstad, "The importance of FeCO3 supersaturation on the CO2 corrosion of carbon steels," *CORROSION/92*, paper no. 14, (1992).

2. E.W.J. Van Hunnik, B.F. Pots, E.L.J.A. Hendriksen, "The formation of protective FeCO3 corrosion product layers in CO2 corrosion," *CORROSION/96,* paper no. 6 (1996).

3. J. Crolet, N. Thevenot, S. Nesic, "Role of conductive corrosion products on the protectiveness of corrosion layers," *CORROSION/96*, paper no. 4, (1996).

4. D. Delafosse, B. Bayle, C. Bosch, "The roles of crack-tip plasticity, anodic dissolution and hydrogen in SCC of mild and C-Mn steels," *Environment-Induced Cracking of Materials,* (2008):*p.* 267-278.

5. C.Bosch, D. Delafosse, X. Longaygue, "Effects of strain and trapping on hydrogen-induced cracking in high strength low alloy steels," *EUROCORR 2010,* (Moscow, Russia, 2010), p. 13-17.

6. H. Cialone, R.J. Asaro, "The role of hydrogen in the ductile fracture of plain carbon steels," *Metallurgical Transactions A,* 10 (1979): p. 367-375.

7. D.G. Enos, J.R. Scully, "A Critical-Strain Criterion for Hydrogen Embrittlement of Cold-Drawn. Ultrafine Pearlitic Steel," *Metallurgical and Materials Transactions A,* 33A (2002): p. 1151 - 1166.

8. R.A. Oriani, P.H. Josephic, "Hydrogen-enhanced nucleation of microcavities in AISI 1045 steel," *Scripta Metallurgica,* 13 (1979): p. 469-471.

9. R. Garber, I.M. Bernstein, A.W.Thompson, "Hydrogen assisted ductile fracture of spheroidized carbon steels," *Metallurgical Transactions A,* 12 (1981): p. 225-234.

10. F.P. Ford, *Corrosion sous contrainte. Phénoménologie et mécanismes* (Les Ulis, France: les éditions de a physique, 1990).

11. R. Troiano, "The role of hydrogen and other interstitials in the mechanical behavior of metals," *Transactions of the ASM,* 52 (1960): p. 54-79.